

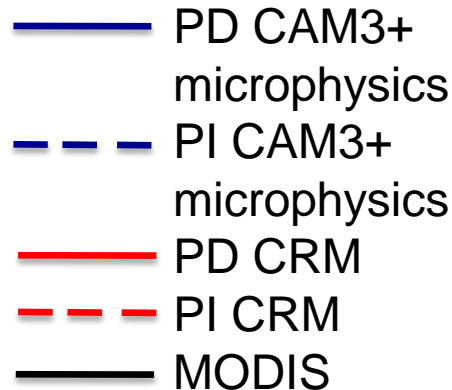
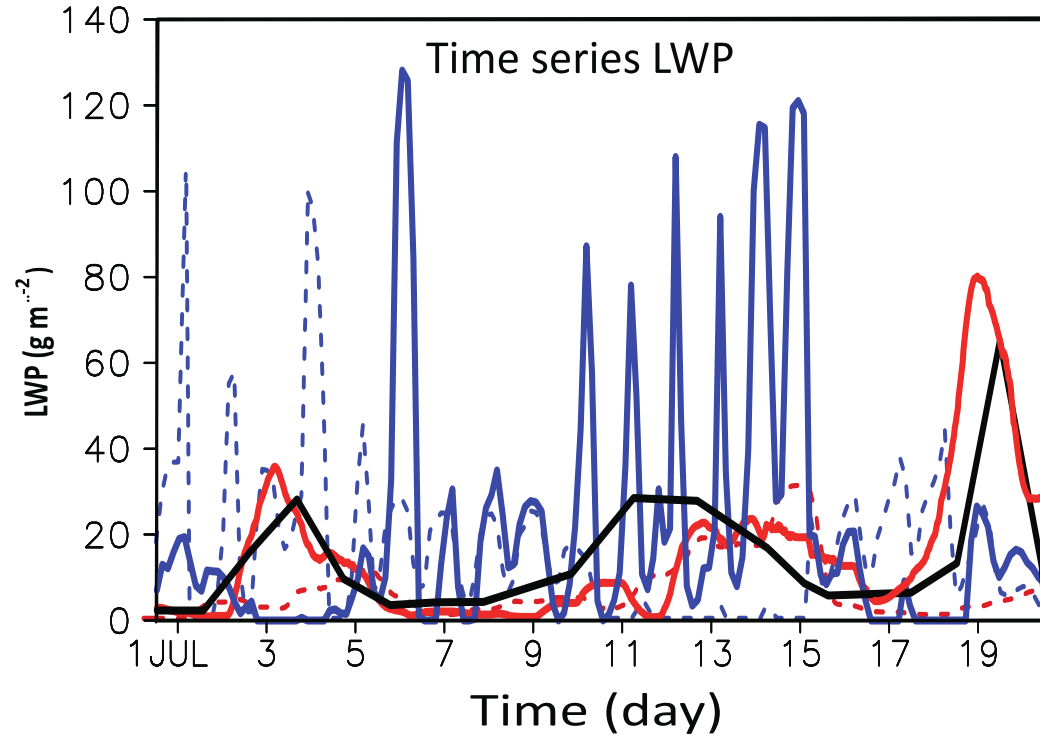
A computationally efficient finite
volume hydrostatic/non-hydrostatic
hybrid model with a vertical
Lagrangian coordinate

Joyce E. Penner, Xi Chen, Natalia
Andronova, Bram van Leer, Quentin
Stout, Denny Vandenberg

University of Michigan
DOE Climate Program
September 19 – 22, 2011

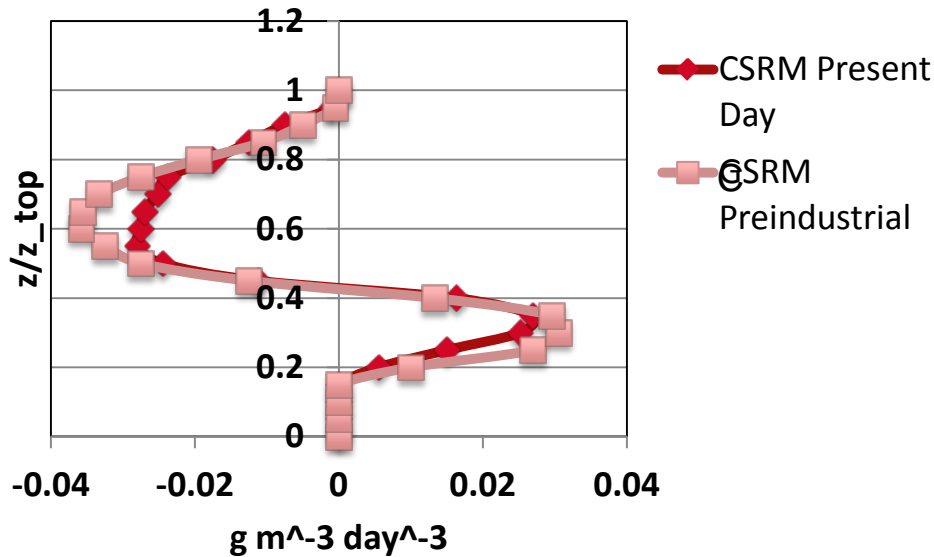
Aerosol-cloud interactions

- Large scale hydrostatic models differ significantly in their predictions relative to non-hydrostatic cloud resolving models



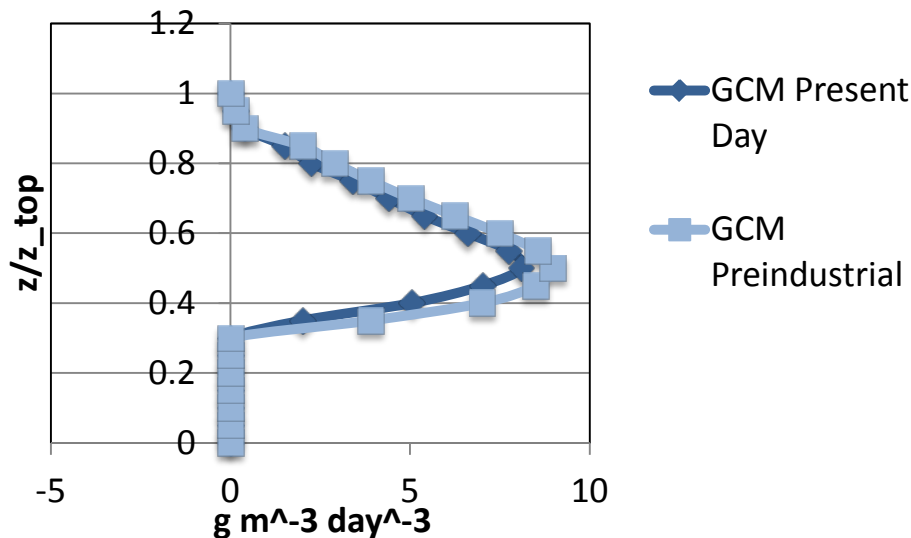
Role of representation of microphysics:

CSRM: change from sedimentation

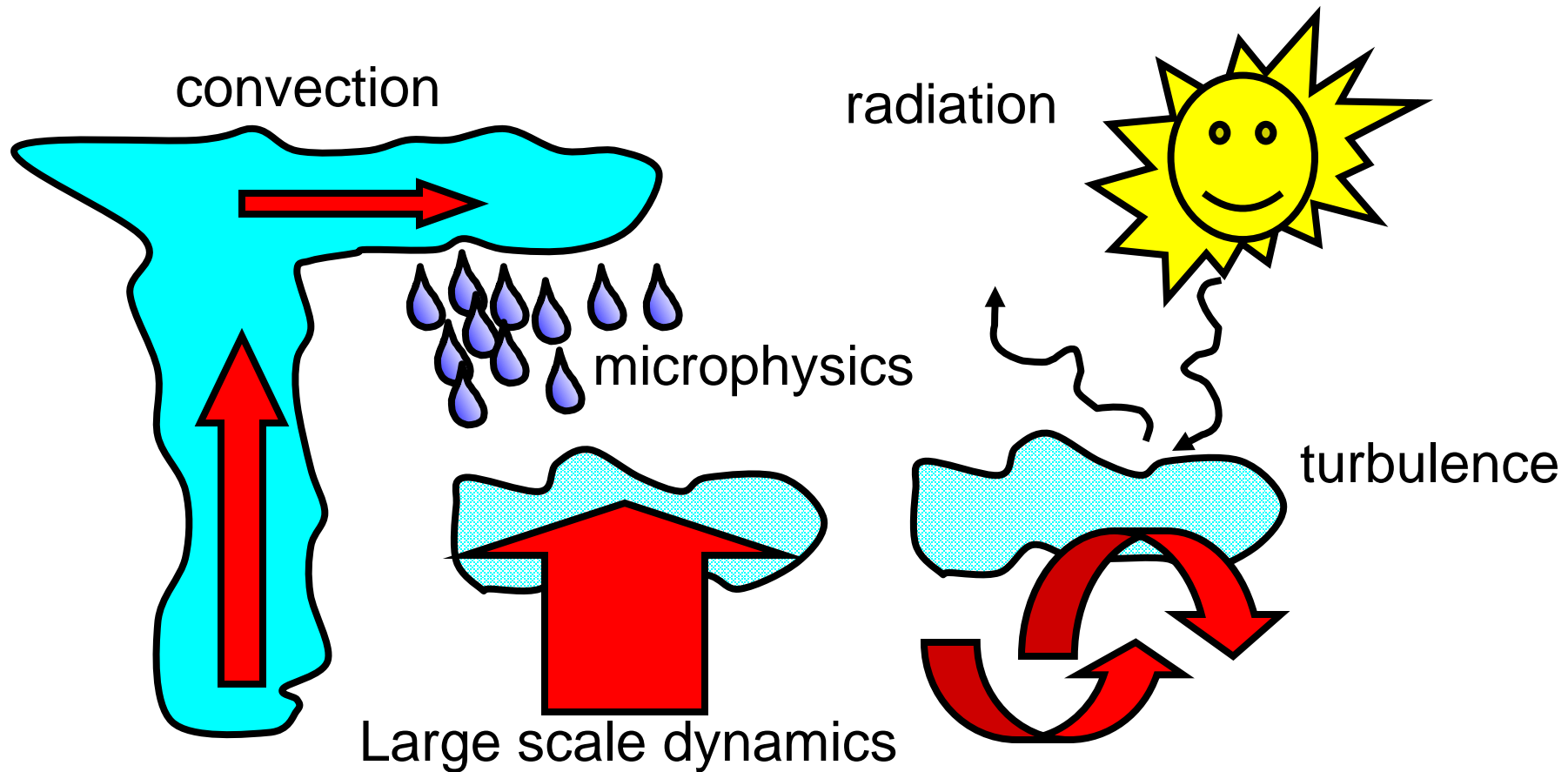


The CRM includes a 2-bin representation of cloud size, allowing particles to fall below cloud base and evaporate. This promotes a decoupling between the surface and cloud layer, in part, allowing cumulus clouds to develop near the end of the simulation in the CSRM.

GCM: loss of cloud liquid to rain



Clouds in GCM - What are the problems ?



Clouds are the result of **complex interactions** between a large number of processes

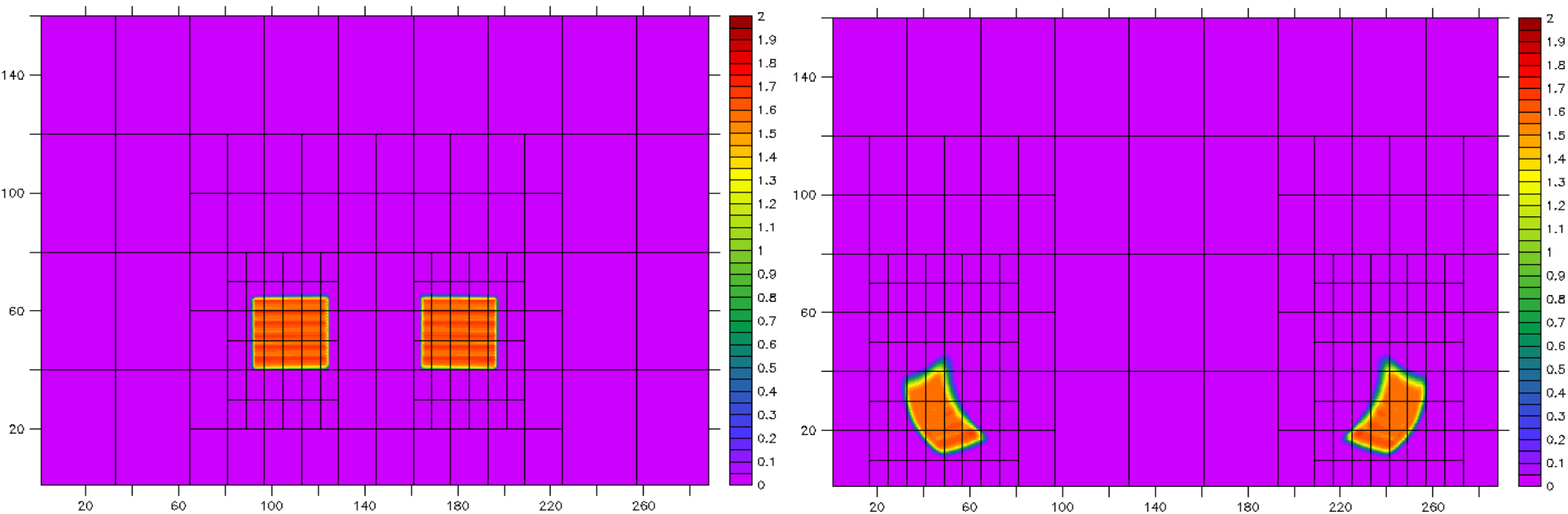
Hydrostatic vs Non-hydrostatic Dynamical Cores

- Resolving aerosol-cloud interactions for large scale clouds requires horizontal resolutions of order 50 m: Non-hydrostatic dynamics
- But large scale motions are resolved using the computationally more efficient hydrostatic dynamics
- Goal of this project was aimed at coupling these two regimes using adaptive grid refinement

Work needed to realize this goal

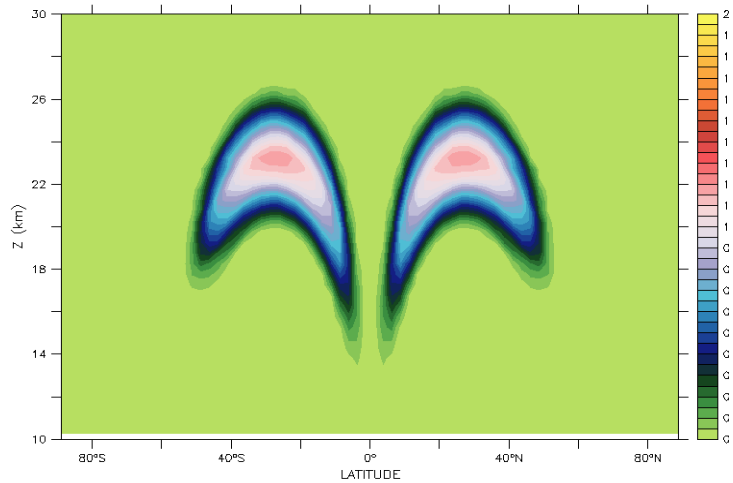
- Build a library that can account for adaptive mesh refinement changing resolution (both horizontally and vertically): **ABLCarT library**
- Test that adaptation within the hydrostatic regime
- Build an efficient non-hydrostatic model using a mass-based vertical coordinate that could seamlessly mesh with the Lin-Rood hydrostatic core
- Join these two models and demonstrate solutions

Test tracer distribution with fixed winds after 1 day with 2 levels of refinement:

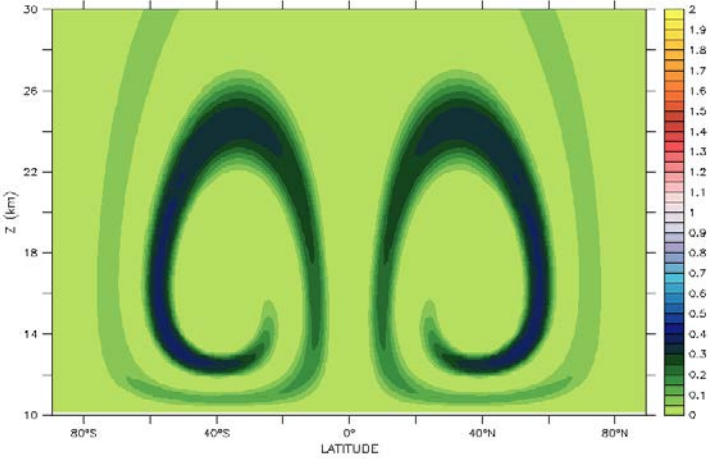
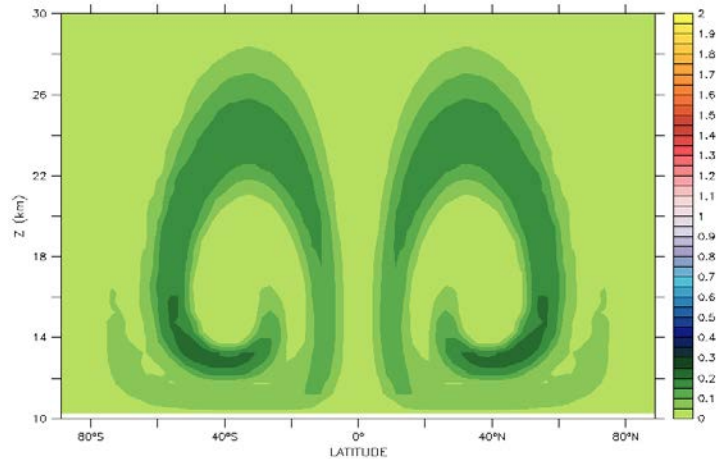
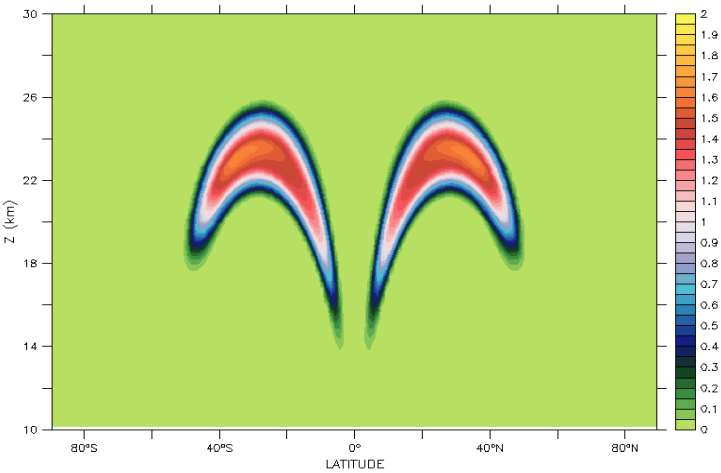


Demonstrate tracer solution using fully vertically-adaptive library

72x40 resolution, no refinement:

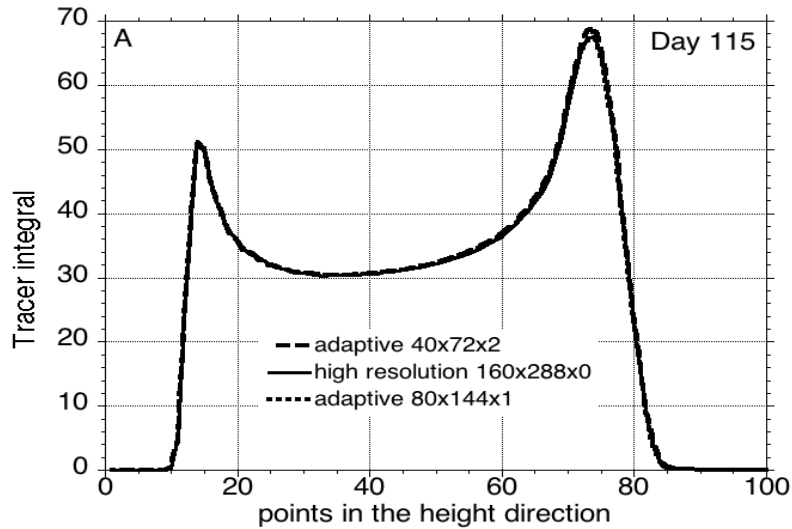


72x40x2 resolution, 2 levels refinement:

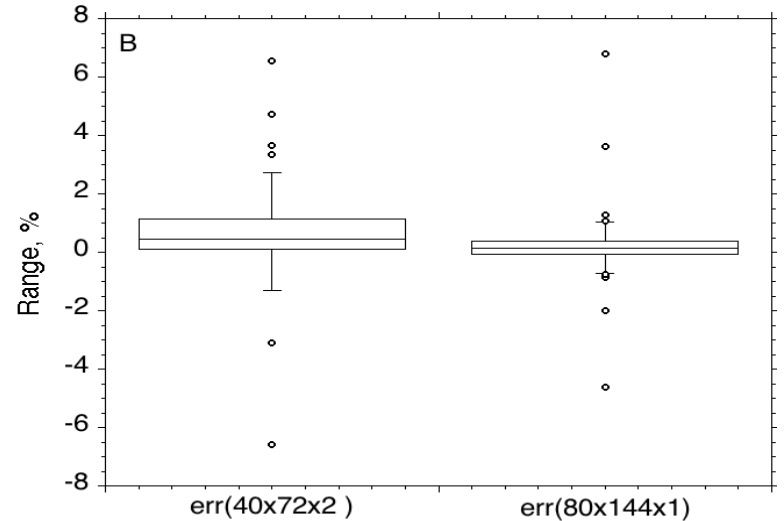


Errors relative to high resolution run:

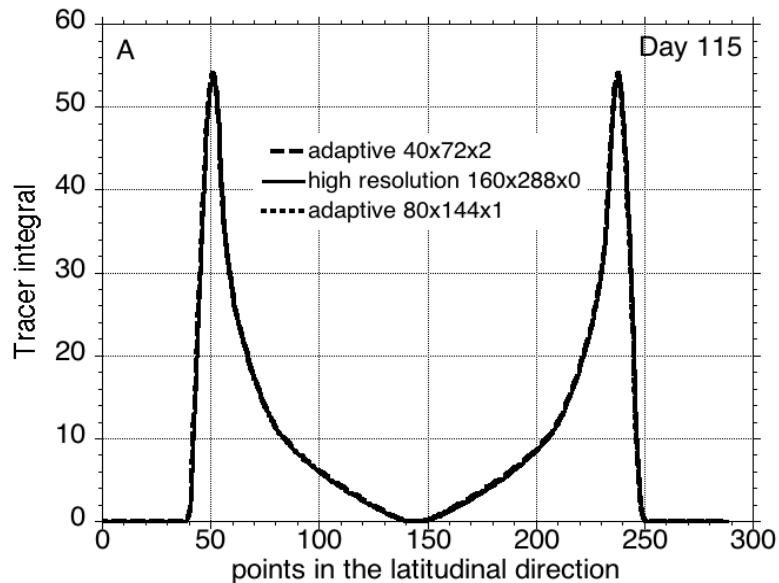
Horizontal integral of tracer distribution



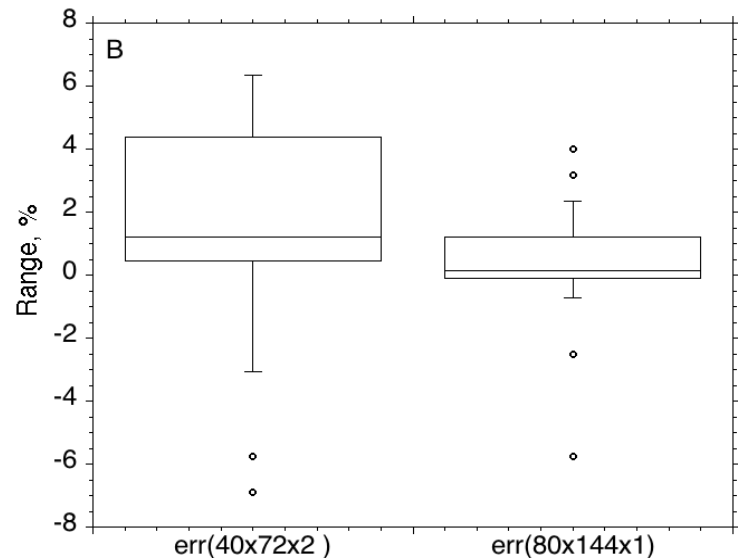
Errors relative to high resolution run:



Vertical integral of tracer distribution

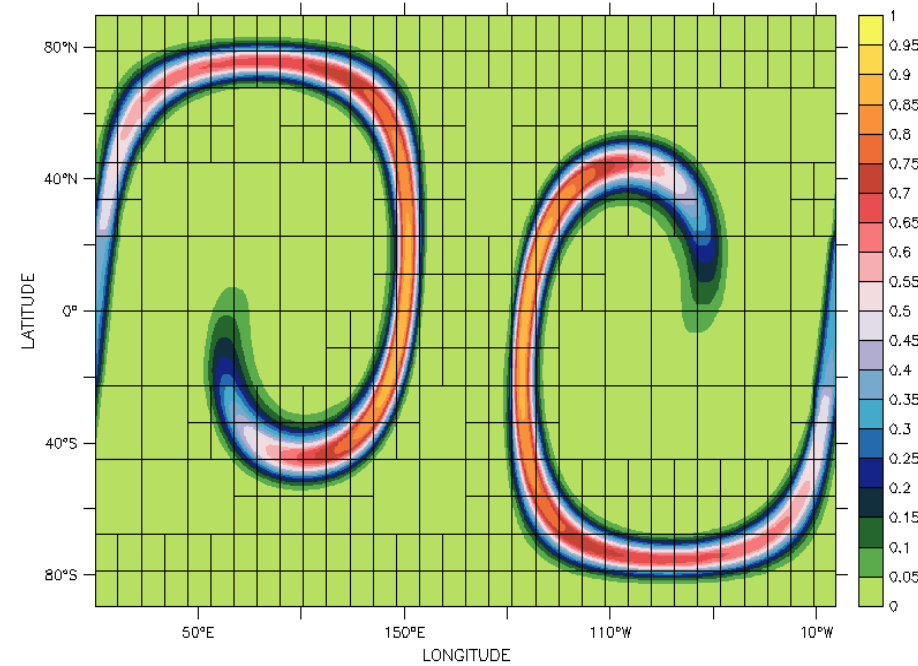
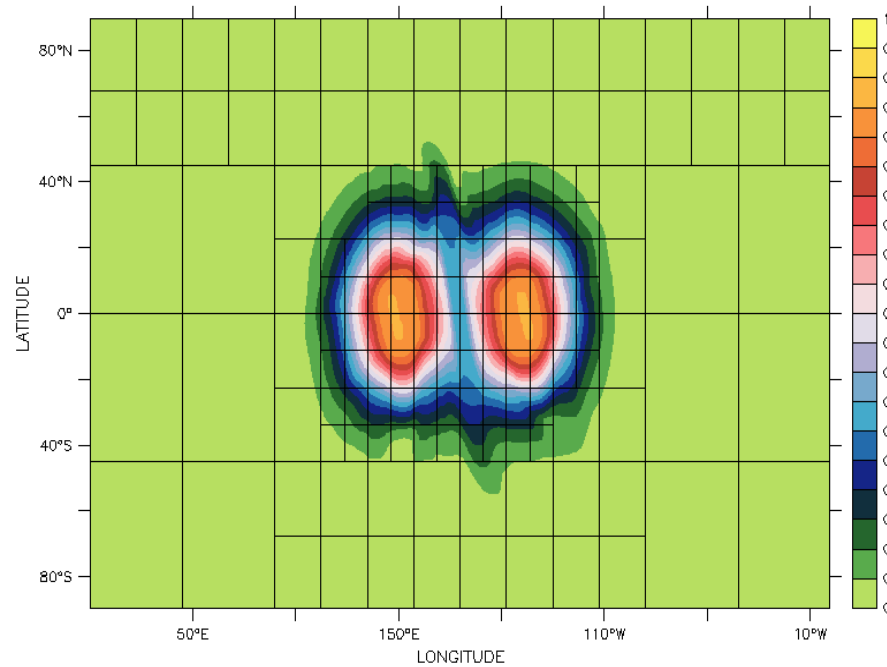


Errors relative to high resolution run:



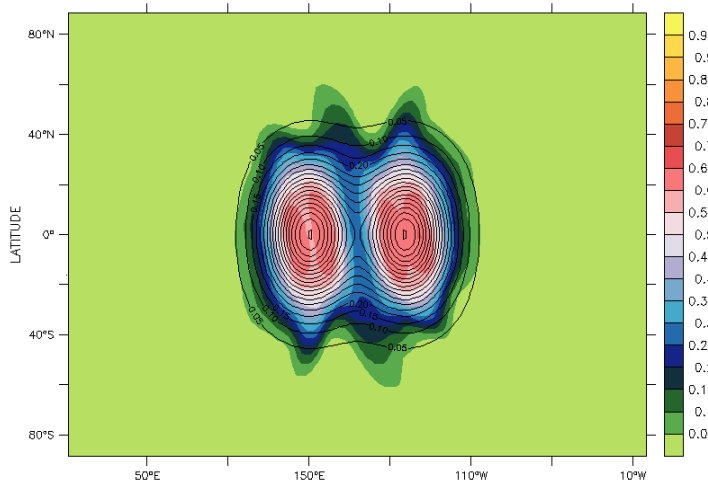
Participated in NCAR tracer distribution tests: Workshop: March 2011

Guassian Hill at full simulation time: Guassian Hill at $\frac{1}{2}$ simulation time:

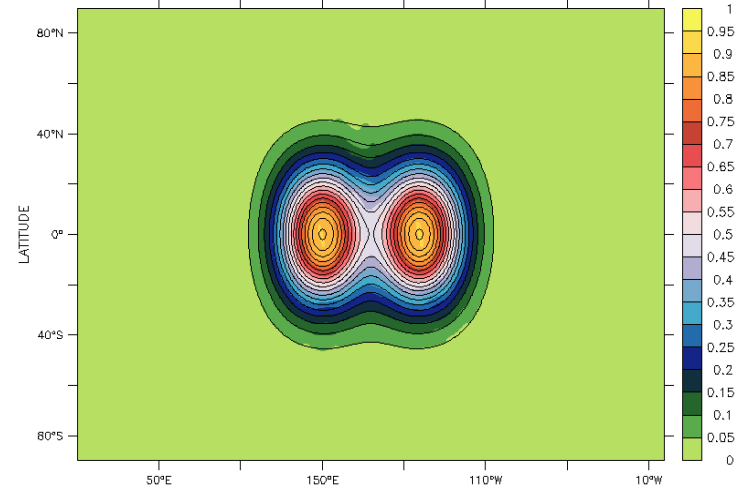


Demonstrate both Gaussian Hill and Slotted Cylinder tests

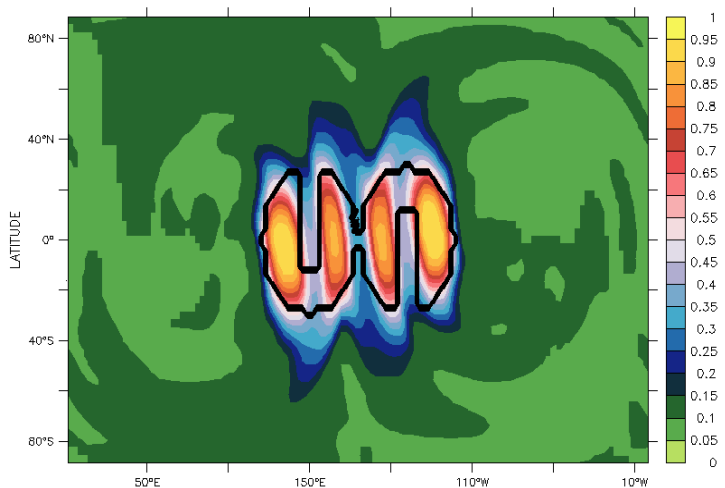
Gaussian Hill, no adaptation (40x80x0)



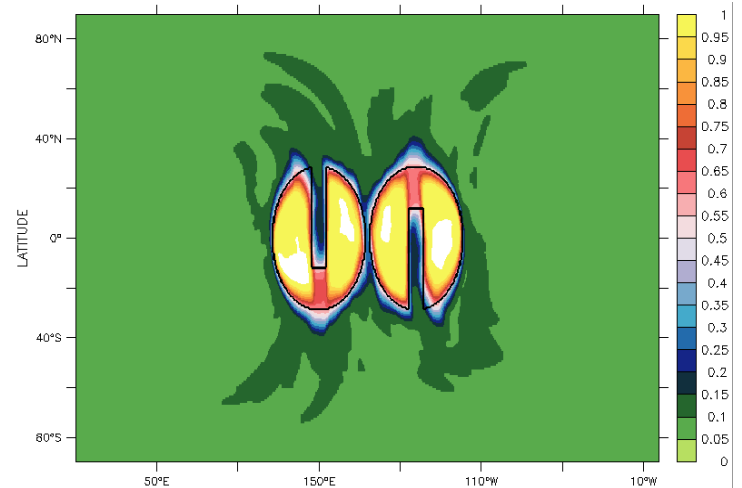
Gaussian Hill, 2 levels adaptation (40x80x2)



Slotted Cylinders, no adaptation (40x80x0)

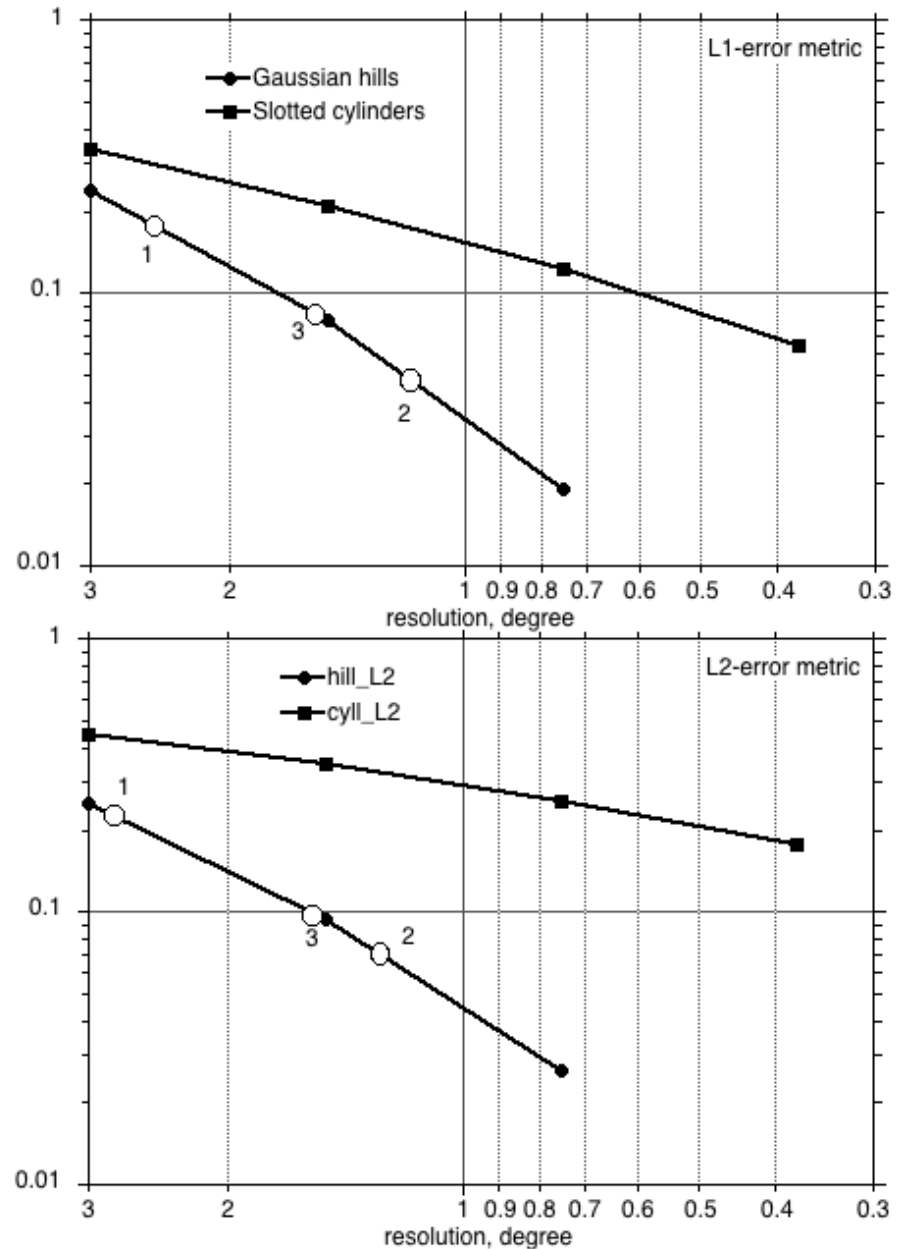


Slotted Cylinders, 2 levels adaptation (40x80x2)



L1 and L2 metrics show improvement with higher resolution: open circles are adaptive runs with different adaptation criteria

$$L_1 = \frac{|\mu - \mu_a|}{|\mu_a|}, \quad L_2 = \frac{(\mu - \mu_a)^2}{(\mu_a)^2}$$



Development of mass-based Lagrangian vertical coordinate in non-hydrostatic dynamical core

$$\pi = \delta p^* = -\rho g \delta z = -\rho \delta \Phi$$

π = mass per unit length within the Lagrangian FV

P^* = hydrostatic pressure

p = full pressure

ρ = atmospheric density

g = gravity,

Φ = geopotential,

Vertical momentum equation:

$$\frac{\partial \pi w}{\partial t} + \frac{\partial \pi w u}{\partial x} = g \delta p'$$

perturbation:

$$\frac{\partial \Phi}{\partial t} + u \frac{\partial \Phi}{\partial x} = w g$$

$$p = \left(-\frac{R\Theta}{\delta \Phi} \right)^\gamma$$

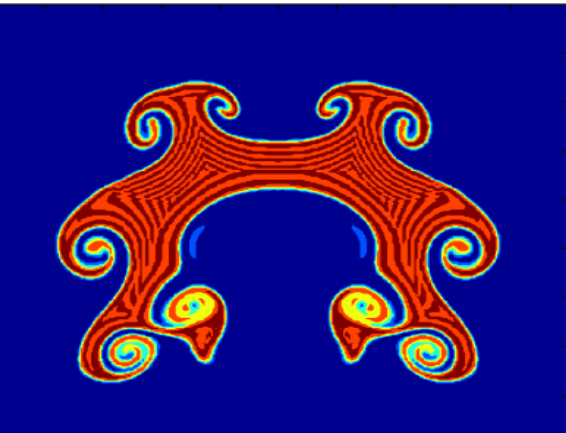
Non-hydrostatic pressure

$$\delta p' = \delta p - \pi$$

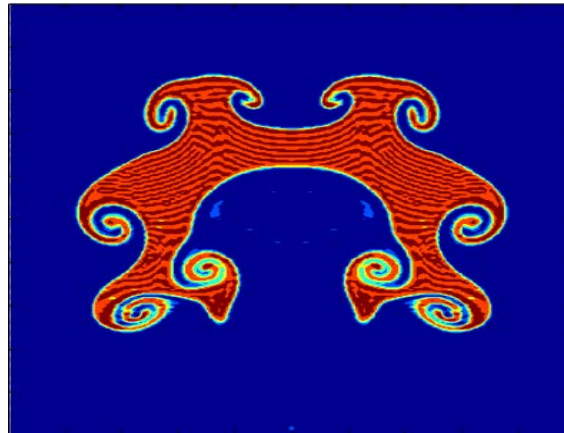
Testing of Lagrangian vertical coordinate using a rising uniform potential temperature bubble perturbation

After 10 minutes

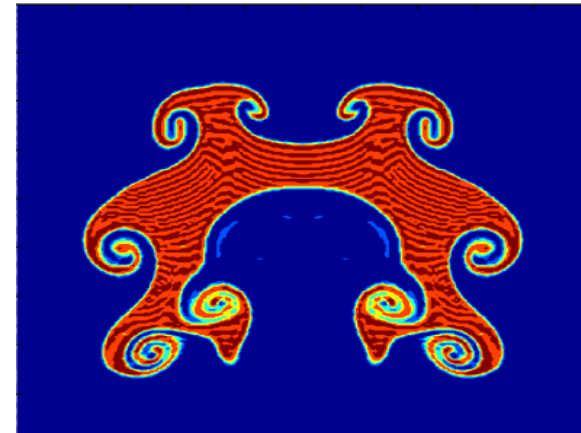
Eulerian: $dx = 10$



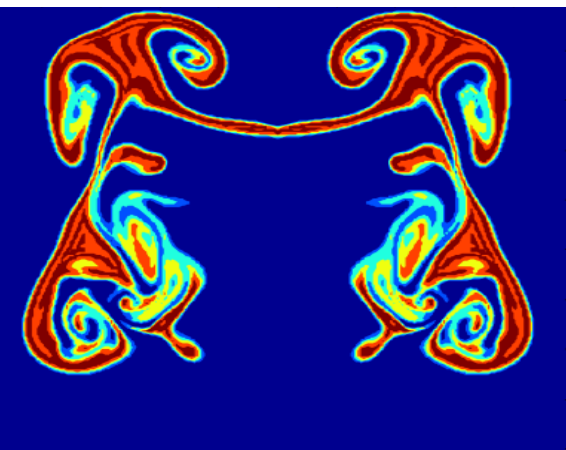
Lagrangian:
Full Riemann solver



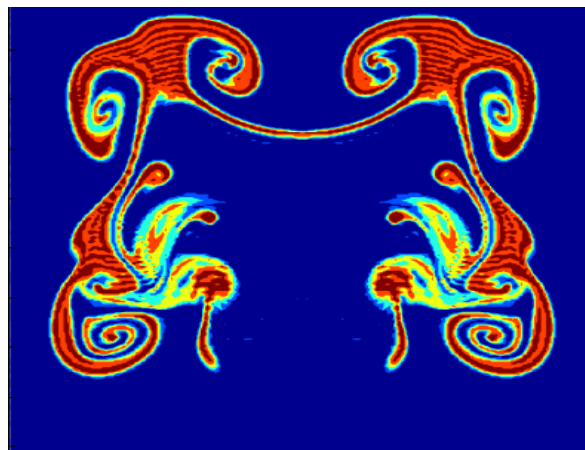
Lagrangian:
Fast Riemann solver



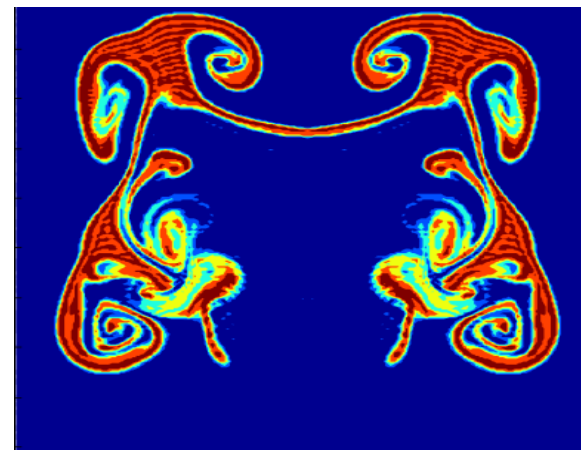
Eulerian: $dx = 5$



Lagrangian:
Full Riemann solver



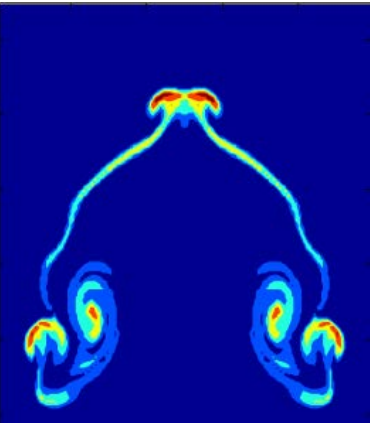
Lagrangian:
Fast Riemann solver



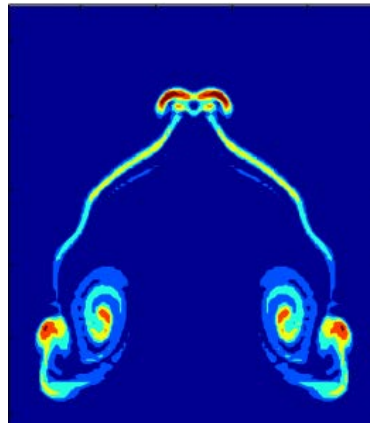
Testing of Lagrangian vertical coordinate using a rising Gaussian potential temperature bubble perturbation

After 18 minutes

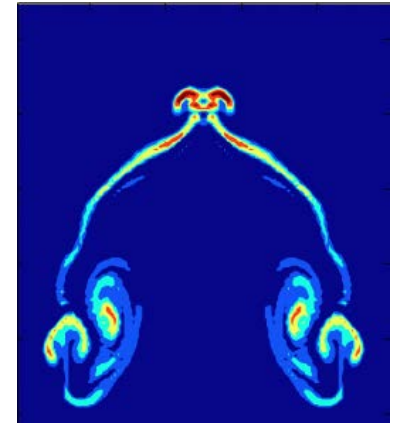
Eulerian: $dx = 10$



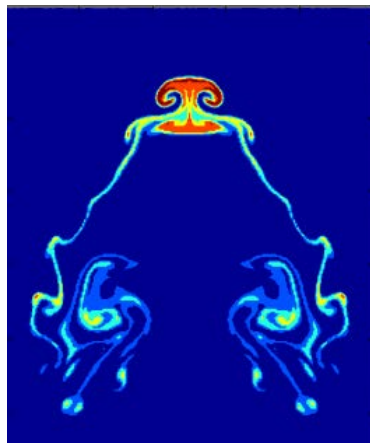
Lagrangian:
Full Riemann solver



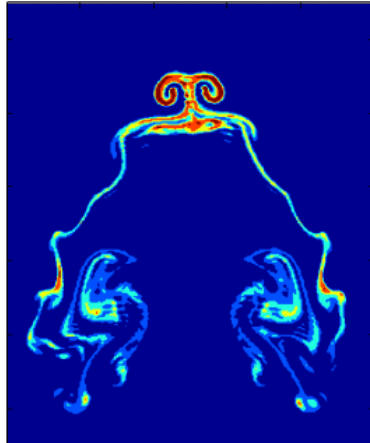
Lagrangian:
Fast Riemann solver



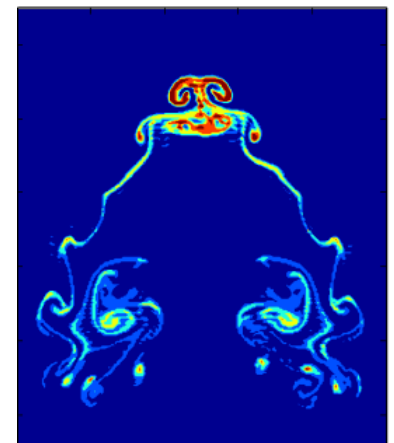
Eulerian: $dx = 5$



Lagrangian:
Full Riemann solver

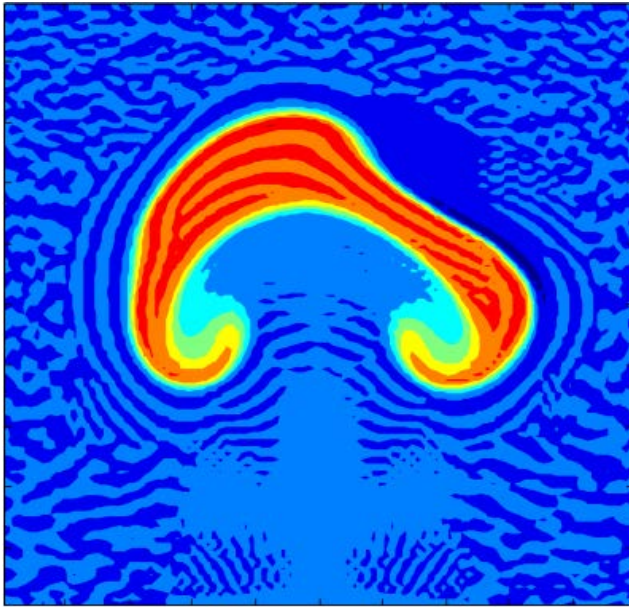


Lagrangian:
Fast Riemann solver

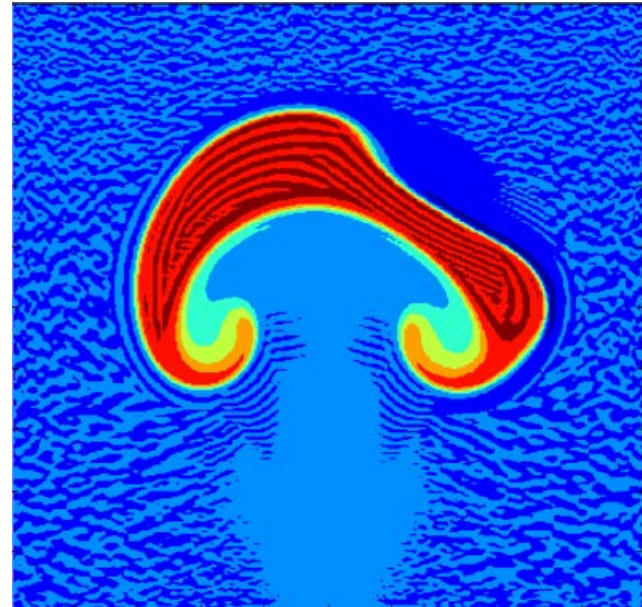


Interaction of warm and cold bubbles:

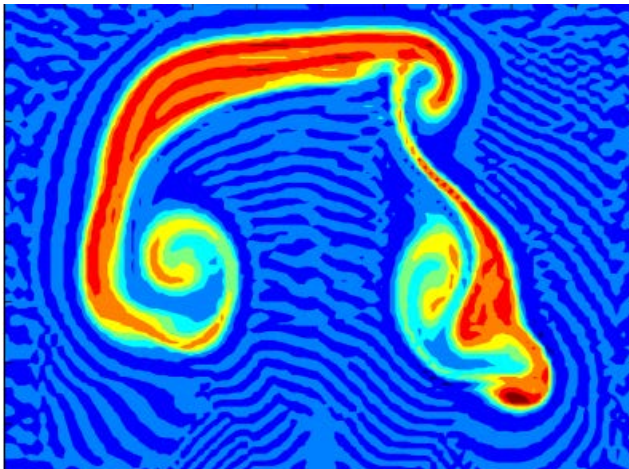
$dx = 10$ m; 7 minutes



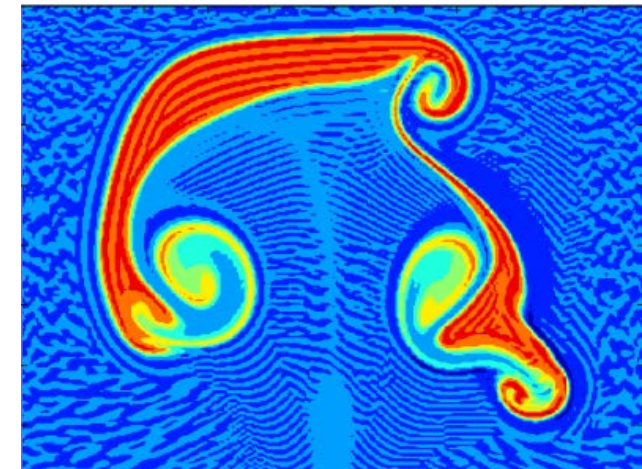
$dx = 5$ m; 7 minutes



$dx = 10$ m; 10 minutes

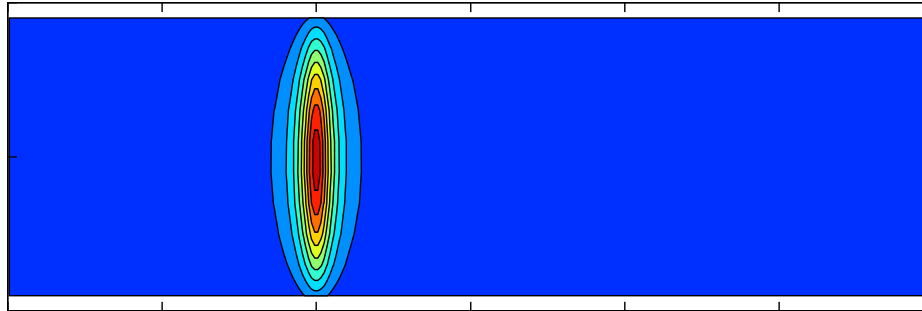


$dx = 5$ m; 10 minutes

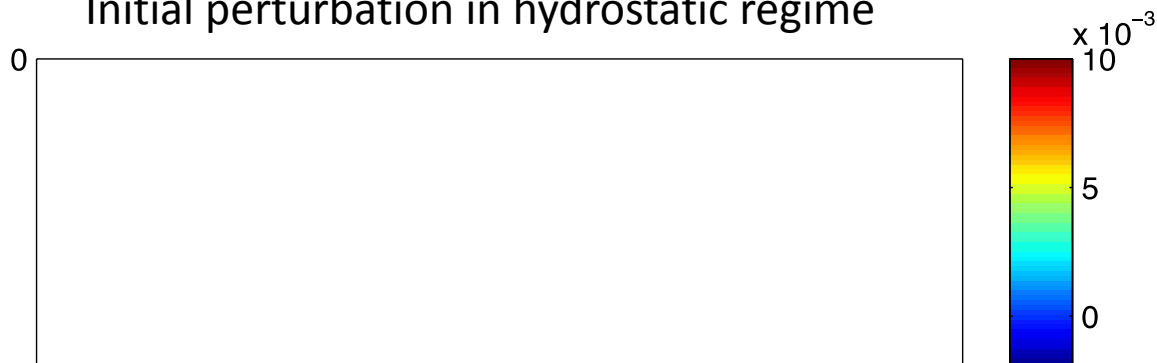


Gravity wave propagation test going from hydrostatic to non-hydrostatic and vica versa: Potential temperature perturbation

Initial perturbation in non-hydrostatic regime

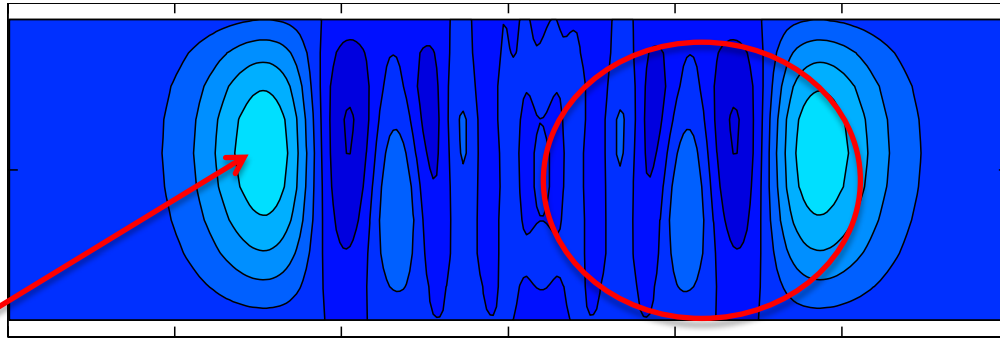


Initial perturbation in hydrostatic regime



Gravity wave propagation in pure non-hydrostatic or hydrostatic regime:

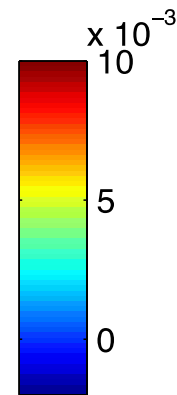
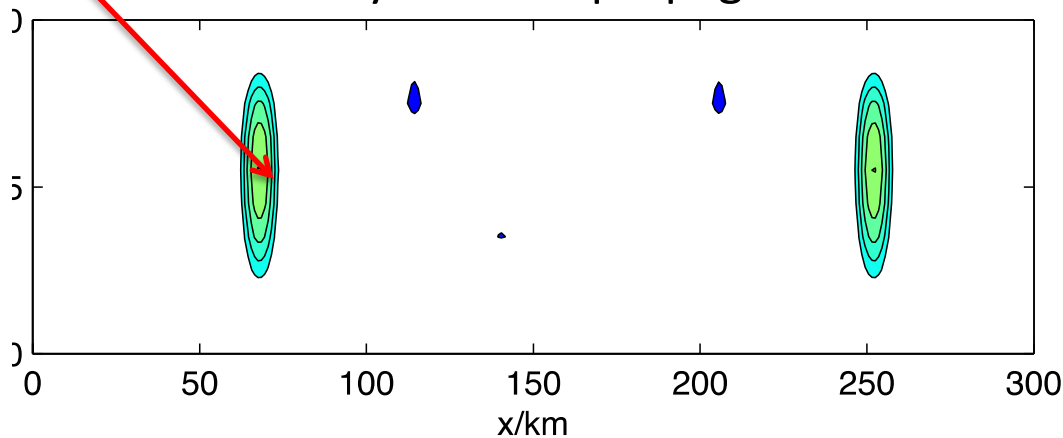
Pure non-hydrostatic propagation



Development of oscillations due to excitation of vertical velocities

Formation of asymmetric bubble in non-hydrostatic region is similar to analytic solution (but may need higher resolution)

Pure hydrostatic propagation



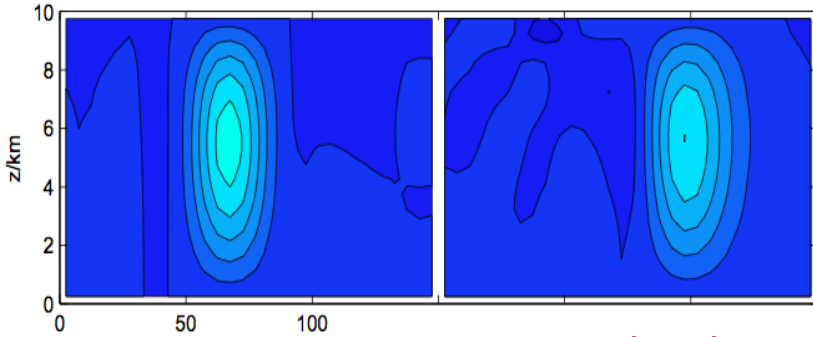
dx=dz=1000m

Gravity wave propagation test going from hydrostatic to non-hydrostatic and vica versa: Perturbation starts on left side of white line

5000 x 500 m

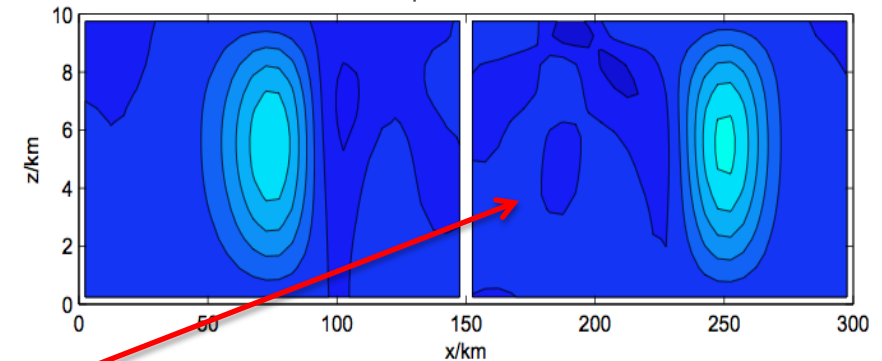
Hydrostatic regime

Non-hydrostatic



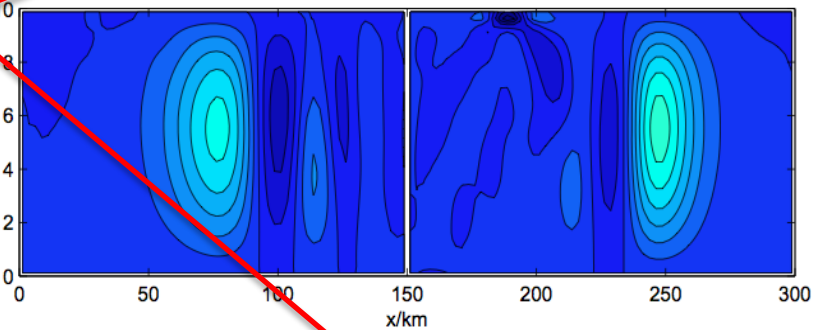
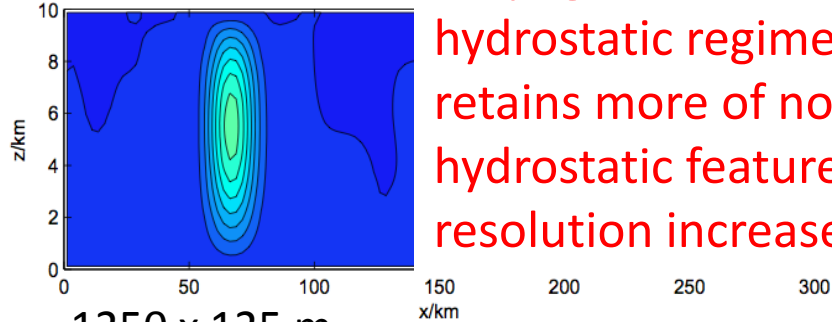
Non-hydrostatic

Hydrostatic

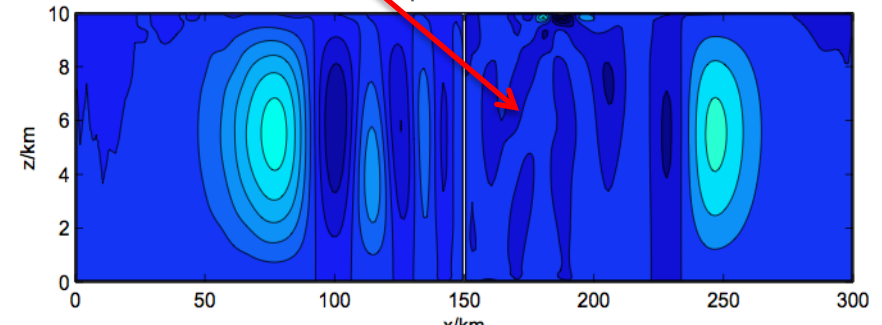
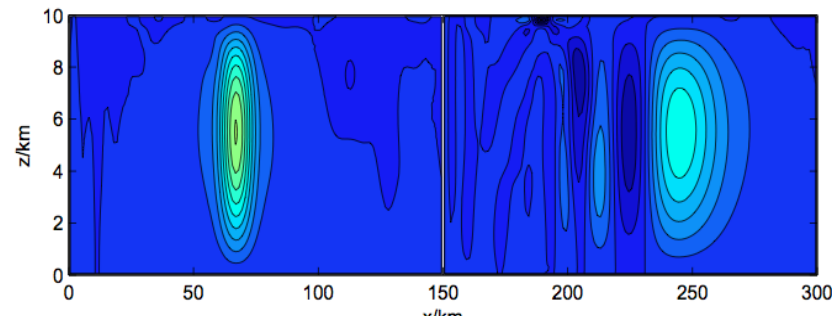


2500 x 250 m

Propagation into hydrostatic regime retains more of non-hydrostatic features as resolution increases.



1250 x 125 m



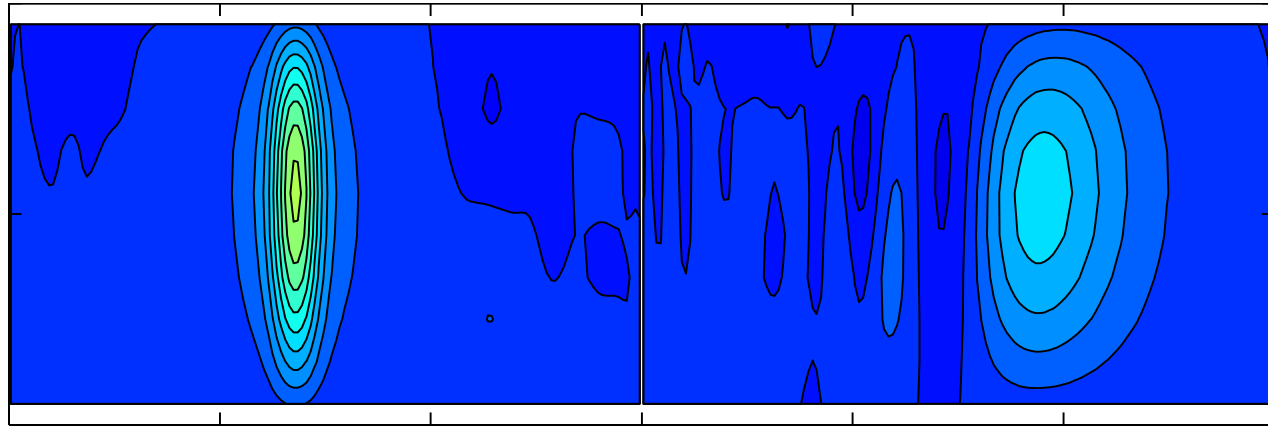
Gravity wave propagation test going from hydrostatic to non-hydrostatic with change of resolution at boundary

$dx=dz=1000$ m

Hydrostatic regime

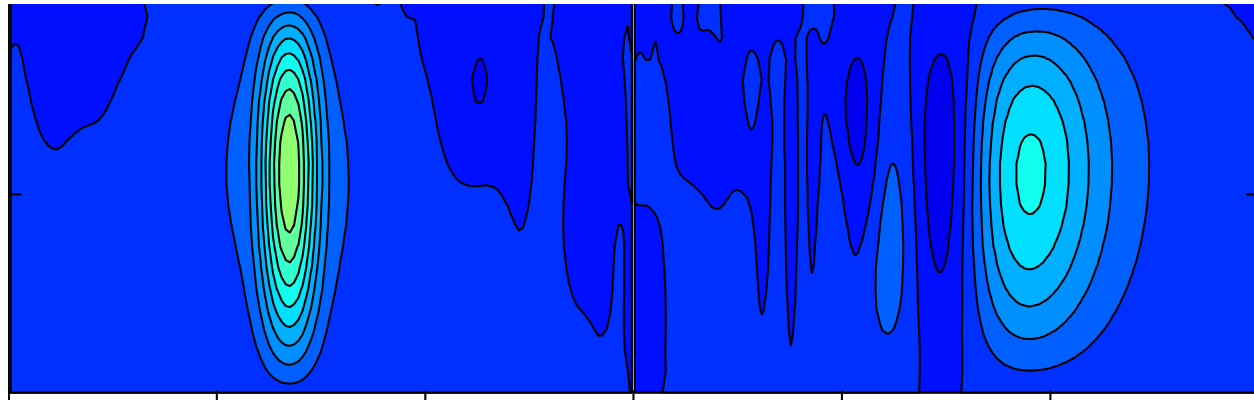
Non-hydrostatic

A-Core
for both
sides



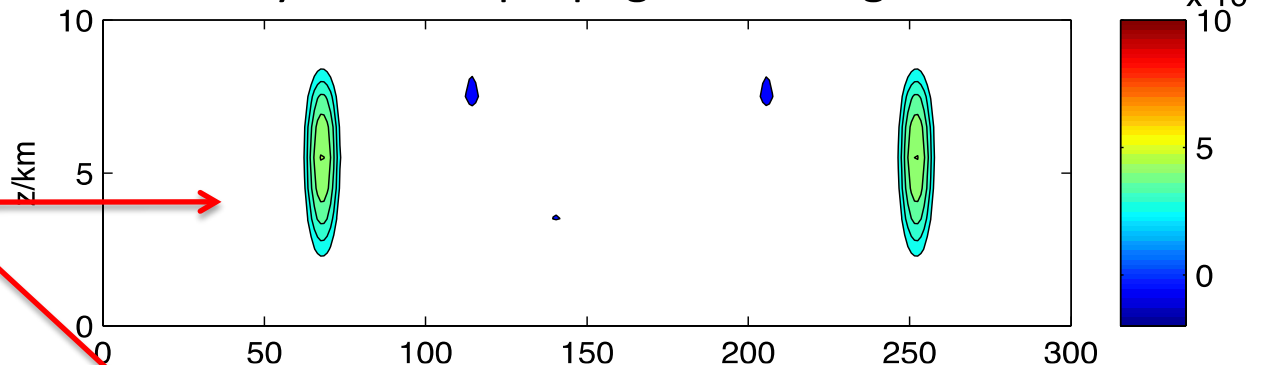
$dx=1000$, $dz=500$ in Hydrostatic; $dx=500$, $dz=500$ m in Non-hydrostatic

Reflection
is minimal
when only
horizontal
resolution
changes



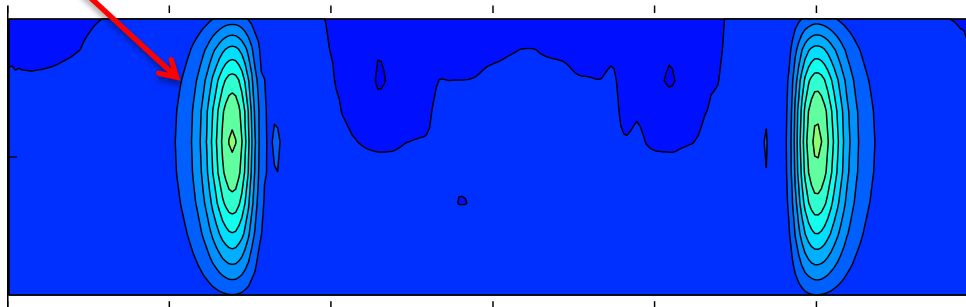
Gravity wave propagation test in pure hydrostatic regime using A vs C-D core:

Pure hydrostatic propagation using A core



Asymmetric bubble forms in CD core version which is similar analytic solution.

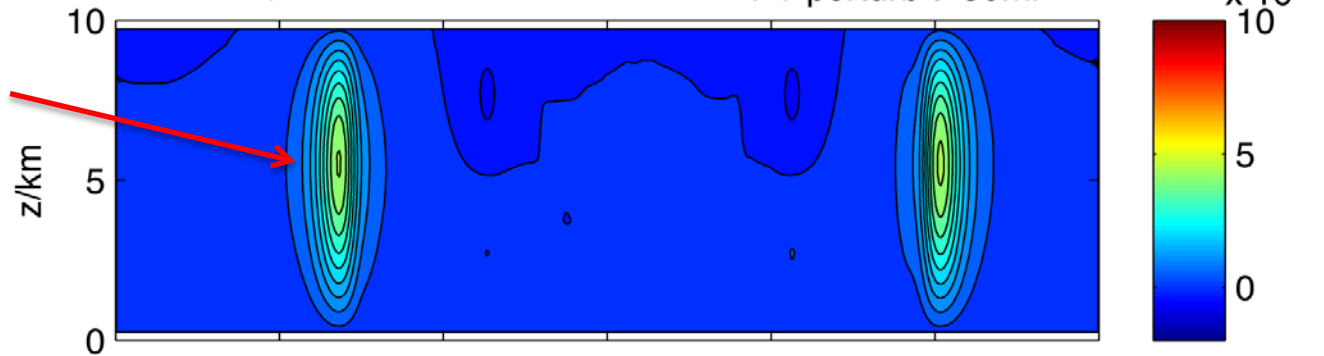
Pure hydrostatic propagation using CD core



CD Core is still asymmetric
If higher resolution is used: Skamarock and Klemp solution is asymmetric.

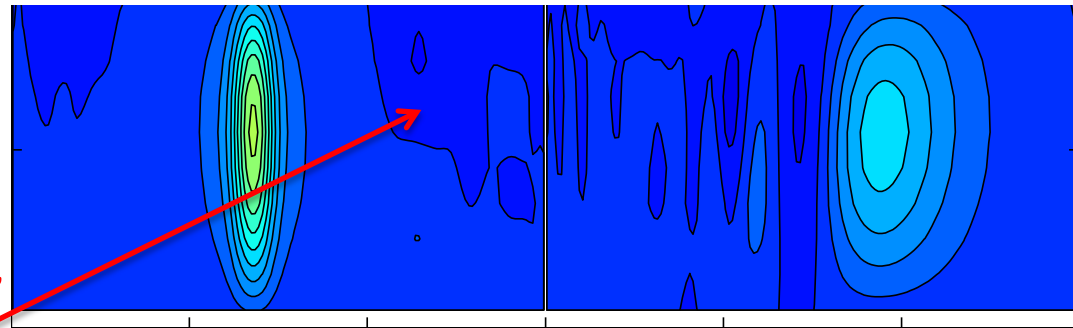
CD core; $dx=dz=500$

PT perturb $t=50\text{mi}$

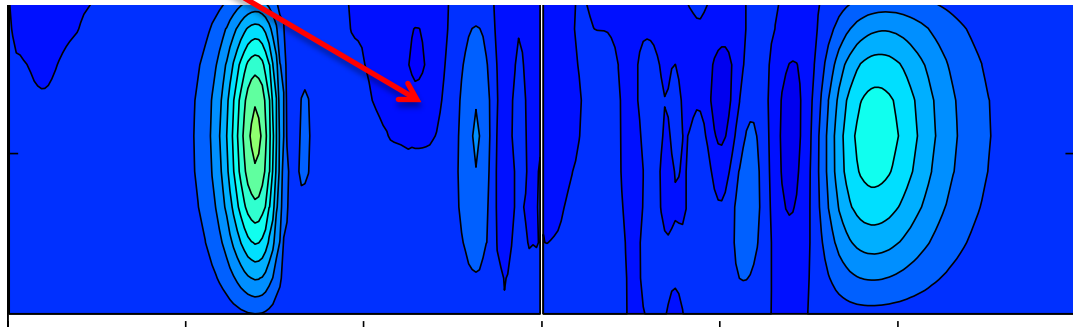


Gravity wave propagation test from hydrostatic to non-hydrostatic regime using pure A-core vs C-D to A-core:

A-Core hydrostatic to A-Core non-hydrostatic



CD-Core hydrostatic to A-Core non-hydrostatic



Larger "contamination"
of solution in
hydrostatic region
in CD to A-Core
treatment

Conclusions and next steps

- We have developed a fast, efficient code with a computational library that allows us to change physics and resolution using adaptive mesh refinement
- Tests for changing resolution in A core and connecting CD to A core demonstrate that we are nearing completion of the development of a dynamical core capable of going from the Lin-Rood treatment in CAM5 to a fully non-hydrostatic treatment
- Next step (next proposal): Add water substance to the model so that it may be joined to CAM
- Next step (Mark Taylor and Paul Ullrich): Add our mass-based vertical non-hydrostatic treatment to HOMME dynamical core